QUANTITATIVE SPECTROSCOPY OF HOT MASSIVE STARS

Lecture III: Spectral Diagnostics II

Brankica Kubátová

Astronomický ústav AV ČR

Selected chapters on astrophysics

Astronomical Institute
Faculty of Mathematics and Physics, Charles University

November 30, 2022, Prague

Determination of the effective temperature

Optical diagnostics

- T_{eff} is derived using the ionization balance method (e.g. Herrero et al. 1992, Puls et al. 1996, Martins et al. 2002).
- He I 4471 and He II 4542 lines - the most reliable indicators for O and WR stars (complementary lines: He I 4026, He I 4388, He I 4712, He I 4920, He II 4200, He II 5412).
- H_α and He II 4686 are contaminated by wind; He I singlet lines are sensitive to line–blanketing effects.
- For $T_{eff} < 27000$ K (mid- and late-B stars) the Si ionization balance is used (Si II 4124-31, Si III 4552-67-74, Si III 5738, Si IV 4089, Si IV 4116)
- Typical uncertainties: 500-2000 K depending on the quality of the observational data and on the temperature itself

Determination of the effective temperature

Optic

Herrero

tors

, He I

glet

ion

38, Si

ality

f

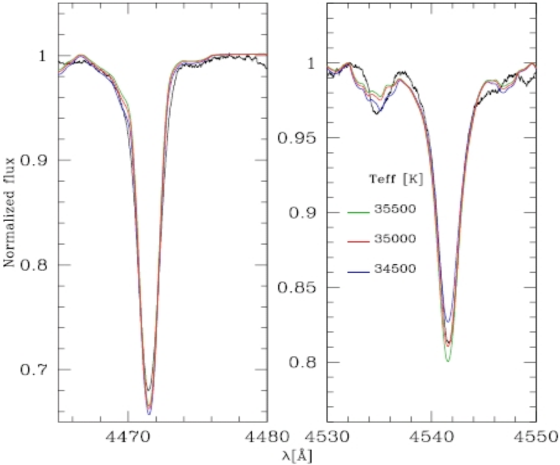

From Martins, 2011

Determination of the effective temperature

Optical diagnostics

- T_{eff} is derived using the ionization balance method (e.g. Herrero et al. 1992, Puls et al. 1996, Martins et al. 2002).
- He I 4471 and He II 4542 lines - the most reliable indicators for O and WR stars (complementary lines: He I 4026, He I 4388, He I 4712, He I 4920, He II 4200, He II 5412).
- H_α and He II 4686 are contaminated by wind; He I singlet lines are sensitive to line–blanketing effects.
- For $T_{eff} < 27000$ K (mid- and late-B stars) the Si ionization balance is used (Si II 4124-31, Si III 4552-67-74, Si III 5738, Si IV 4089, Si IV 4116)
- Typical uncertainties: 500-2000 K depending on the quality of the observational data and on the temperature itself

Determination of the effective temperature

IR and UV diagnostics

- The K-band - He I and He II lines are present above $T_{eff} \sim 30000$ K (2.058 μm, 2.112 μm, He II 2.189 μm)
- The strongest He I 2.058 μm depends on line-blanketing effects.
- He I 2.112 μm is preferred although the line is weaker and can be blended with C III/N III emission.
- When only UV spectra are available, the determination of T_{eff} is more difficult - rely on the iron ionization balance (line forest from Fe IV 1600-1630 Å, V 1360-1380 Å, VI 1260-1290 Å).
- The relative strength of Fe line forests provides the best T_{eff} indicator (uncertainties are usually larger than optical determination).
- When possible the C IV 1169 Å to C III 1176 Å line ratio can be used (see Heap et al. 2006).

Determination of the effective temperature

IR and UV di

- The K-b … ove $T_{eff} \sim 30$ … m)
- The str … anketing effects.
- He I 2.1 … eaker and can be
- When … nination of T_{eff} is m … alance (line forest f … 1260-1
- The rel … he best T_{eff} indicat … optical determ
- When … he ratio can be use

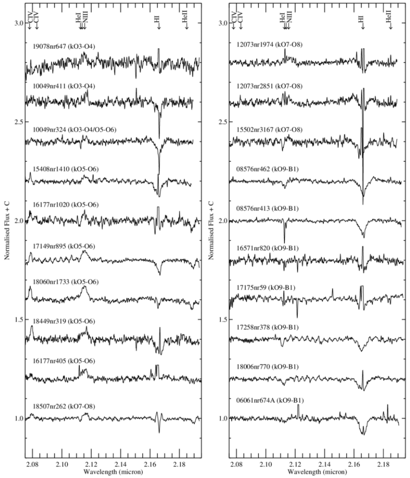

From Bik et al., 2005

Determination of the effective temperature

IR and UV diagnostics

- The K-band - He I and He II lines are present above $T_{eff} \sim 30000$ K (2.058 μm, 2.112 μm, He II 2.189 μm)
- The strongest He I 2.058 μm depends on line-blanketing effects.
- He I 2.112 μm is preferred although the line is weaker and can be blended with C III/N III emission.
- When only UV spectra are available, the determination of T_{eff} is more difficult - rely on the iron ionization balance (line forest from Fe IV 1600-1630 Å, V 1360-1380 Å, VI 1260-1290 Å).
- The relative strength of Fe line forests provides the best T_{eff} indicator (uncertainties are usually larger than optical determination).
- When possible the C IV 1169 Å to C III 1176 Å line ratio can be used (see Heap et al. 2006).

Determination of the effective temperature

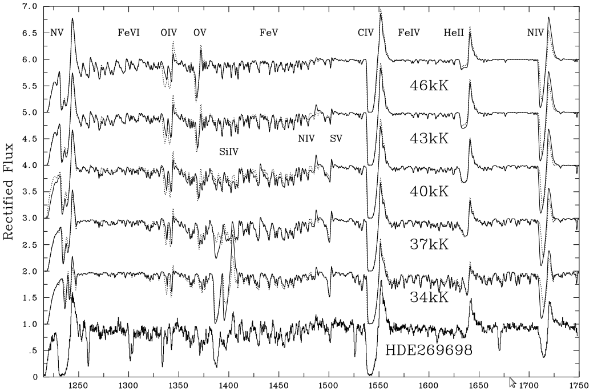

Fig. 7.—Comparison between UV (*HST*) observations of HDE 269698 (O4 Iaf$^+$) and synthetic spectroscopy ($v \sin i$ = 80 km s^{-1}) for a range of stellar temperatures, with mass-loss rates adjusted to reproduce the observed Hα emission profile. Models with processed (*solid lines*) and unprocessed (0.4 $Z_\odot$; *dotted lines*) CNO abundances are indicated for each model. In contrast with the optical, UV P Cygni lines are rather insensitive to temperature and abundance variations. The greatest morphological differences over the temperature range covered are due to the weak iron features—Fe vi $\lambda\lambda$1250–1350, Fe v $\lambda\lambda$1350–1500, and Fe iv $\lambda\lambda$1550–1700. For comparison purposes, the synthetic model is corrected for Lyα at 1215.7Å, with log(H$_2$/cm^{-2}) = 20.7.

From Crowther et al., 2002

Determination of the effective temperature

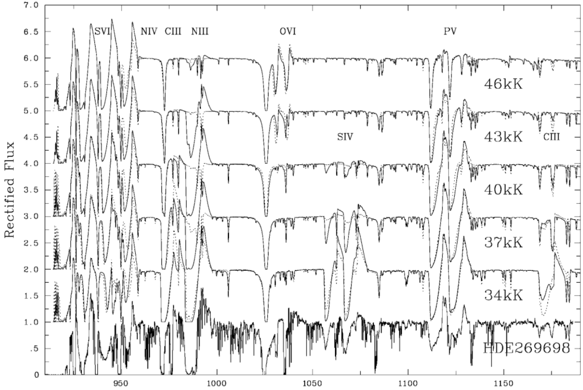

FIG. 8.—Comparison between FUV (*FUSE*) observations of HDE 269698 (O4 Iaf$^+$) and synthetic spectroscopy ($v \sin i = 80$ km s^{-1}) for a range of stellar temperatures, with mass-loss rates again adjusted to reproduce the observed Hα emission profile. Models with processed (*solid lines*) and unprocessed (0.4 $Z_\odot$; *dotted lines*) CNO abundances are indicated for each model. The P Cygni profiles sampled in the *FUSE* spectral range, in contrast with the *HST* range, are very sensitive to temperature and abundances variations, notably C III λ977, N III $\lambda\lambda$989–991, O VI $\lambda\lambda$1032–1038, S IV $\lambda\lambda$1062–1072, P V $\lambda\lambda$1118–1128, and C III λ1175. For comparison purposes, the synthetic model is corrected for the Lyman H I series (principally Lyβ at 1025.7 Å and Lyγ at 972.5 Å) with $\log(H_2/\mathrm{cm}^{-2}) = 20.7$.

From Crowther et al., 2002

Determination of the surface gravity

Optical and IR diagnostics

- Derived from optical spectroscopy - the wings of the Balmer lines broadened by collisional processes (linear Stark effect), stronger in denser atmospheres, i.e. for higher $\log g$.
- The wings of the Balmer lines of H_β, H_γ, and H_δ are the main indicators.
- In the near-IR - the Brackett lines (only the wings have to be considered since they are sensitive to collisional broadening).
- Br γ - the best gravity indicator in the K-band.
- Br10 and Br11 (H-band) can be used as secondary indicators.

Determination of the surface gravity

Optical and IR diagnostics

- Derived from optical spectroscopy - the wings of the Balmer lines broadened by collisional processes (linear Stark effect), stronger in denser atmospheres, i.e. for higher $\log g$.
- The wings of the Balmer lines of H_β, H_γ, and H_δ are the main indicators.
- In the near-IR - the Brackett lines (only the wings have to be considered since they are sensitive to collisional broadening).
- Br γ - the best gravity indicator in the K-band.
- Br10 and Br11 (H-band) can be used as secondary indicators.

Determination of the surface gravity

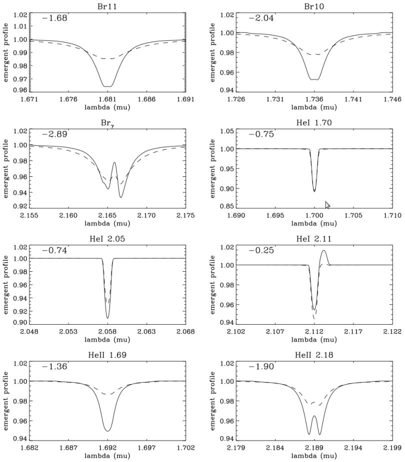

Two atmospheric models: T_{eff}=40.000 K; $\log g$=3.7 (solid) and $\log g$=4.5 (dashed). From Repolust et al., 2005.

Determination of the luminosity

SED fitting

- SED fitting - spectrophotometry ranging from the (far)UV to the infrared is used to adjust the global flux level of atmosphere model.
- There is no need for bolometric corrections.
- The reddening can be derived simultaneously.
- The distance to the star must be known independently.

B. Šurlan et al.: Macroclumping as solution of the discrepancy between Hα and P V mass loss diagnostics for O-type stars

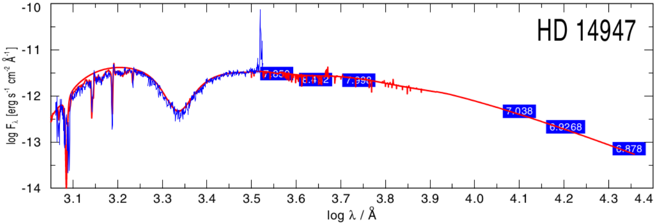

Determination of the surface abundances

Diagnostic lines

- Method consists in comparing synthetic spectra with different abundances to key diagnostic lines.
- Optical studies of OB stars - determination of abundances of C, N, O, Si, Mg (important for wind properties determination).
- The main diagnostics
  - Carbon: CII 4267, CII 6578-82 / CIII 4647-50, CIII 5696 / CIV 5802-12.
  - Nitrogen: NII 3995 / NIII 4510-15 / NIV 4058, NIV 5200 / NV 4605-20.
  - Oxygen: OII 4075, OII 4132, OII 4661 / OIII 5592.
  - Silicon: SiII 4124-31 / SiIII 4552-67-74, SiIII 5738 / SiIV 4089, SiIV 4116.
  - Magnesium: MgII 4481.
- In O and B stars, the determination of surface abundances requires the knowledge of the micro-turbulence velocity - constrained from a few metallic lines.

Determination of the terminal velocity

Saturated UV P-cygni line profiles

- By measuring the position of the "blue" absorption edge.
- $\Delta\lambda$ - frequency of the blue edge minus frequency of the absorbed photon.

$$v_\infty = \frac{\Delta\lambda}{\lambda_0} c$$

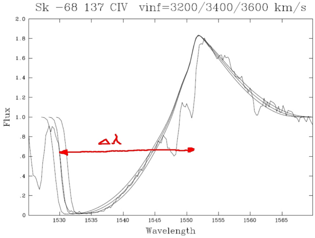

HST FOS spectrum of the LMC O3-star Sk - 68° 137

(from Kudritzki, 1998).

Determination of the terminal velocity

Saturated UV P-cygni line profiles

- Often the blue edges of the absorption trough of strong lines are not well defined - "softening" is interpreted as an indicator for existence of some extra velocity field, caused by additional small-scale or large-scale motions.
- The value v_∞ determined from the "softened" blue edge of the line profile is overestimated.

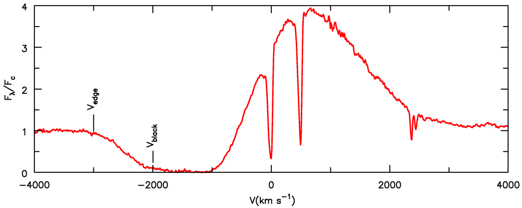

From Howarth et al., 1986.

Determination of the terminal velocity

UV and optical diagnoostics

- **UV diagnostics:** N V 1240, Si IV 1393–1403, C IV 1548–1552, N IV 1718. Additional indicators are found in the FUSE range: O VI 1032-1038, C III 1176.
- **Optical diagnostics:** the Balmer lines and sometimes some He I lines (e.g. He I 4471) can have pure emission or P-Cygni profiles.

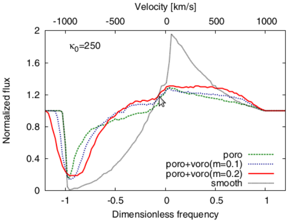

From Šurlan et al., 2012

Mass-loss rate determination

Hα emission

- The Hα emission originates in inner regions of the wind ($\lesssim 2R_*$).
- Observed profiles of the hydrogen Hα line are compared with the theoretical ones - the observed mass loss rate.
- Calculations often based on non-LTE model atmospheres with a given velocity field and core-halo approximation is assume.
- Hα - recombination lines (opacity scales with density square, $\tau \propto \rho^2$).
- Overestimate the mass-loss rate by a factor $\sqrt{f_{cl}}$ if clumping were neglected in the analysis.
- Only sensitive for mass-loss rates above 10^7 $\mathrm{M}_\odot$/yr (Mokiem et al. 2007).
- For weaker winds the NIR regime might provide alternative ρ^2 diagnostics (Najarro et al. 2011).

Mass-loss rate determination

The strengths of UV P-Cygni profiles

- Resonance lines from dominant ions; mainly unsaturated, e.g., Si IV (1394, 1403 Å), P V (1118, 1128 Å).
- Originates in the intermediate region of the wind (10 - 100 R_*).
- The strength of UV resonance lines dependence linearly on density $\rho \propto \dot{M}/(r^2 v_\infty)$.
- The integrated line strength from unsaturated profiles to constrain $\dot{M}$. The product $\dot{M}\, q_i$ can be inferred (q_i - ionization fraction of corresponding ion).
- Phosphorus V problem (Fullerton et al., 2006) - disagreement between the derived mass-loss rates from the P v line and using other methods.

Mass-loss rate determination

Radio and (sub)millimetre continuum emission

- The most reliable method for mass-loss rate measurements, as they are considered to be model-independent.
- It is based on detection of radiation coming from the outermost parts of the wind, where the wind velocity is nearly v_∞ (almost constant).
- The dominant source of radiation is the free-free emission (thermal origin). The assumption of the local thermodynamic equilibrium is valid for this process.
- A mass-loss rate depending on the v_∞, measured radio flux, and the stellar distance (see Panagia & Felli 1975; Wright & Barlow 1975).
- This type of mass-loss rate determination is restricted to closest stars and to the brightest objects.
- Complications due to clumping/porosity (binaries and magnetic fields).

THANK YOU FOR YOUR ATTENTION!

Brankica Kubátová

E-mail: brankica.kubatova@asu.cas.cz
Hompage: http://stelweb.asu.cas.cz/ brankica/